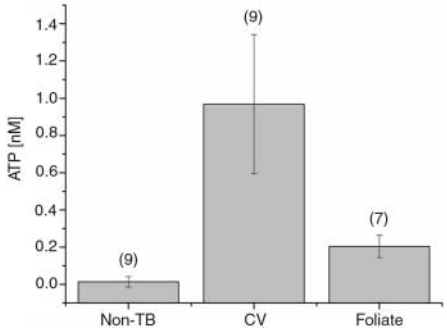


**Fig. 4.** Release of ATP from taste epithelium when stimulated with a bitter mixture containing denatonium and quinine. Nongustatory epithelium (non-TB) and taste bud–bearing epithelial sheets containing either circumvallate (CV) or foliate papillae were placed in an Ussing-type chamber that permits selective application of taste stimuli to the apical membrane. ATP released from the basolateral compartment was collected in the luciferase assay buffer and transferred to the luminometer for measurement of relative light units, which were converted into ATP concentration. Stimulation of taste epithelia with the bitter mixture significantly increases ATP release (mean ± SEM) from CV and foliate tissues relative to non-TB tissue ($P < 0.05$, *t* test).

sensory transmission in this system. Finally, extracellular ATP is rapidly degraded by ecto-ATPases known to be abundantly present in taste buds (*17*–*19*). Thus, ATP meets all the essential criteria for being the major neurotransmitter of the peripheral taste system. Other neuropeptides and transmitters observed within taste buds (*1*, *2*, *20*, *21*) likely play a modulatory role or may be crucial for intragemmal communication among the different types of taste cells.

### References and Notes


1. Y. J. Huang *et al.*, *J. Neurosci.* **25**, 843 (2005).
2. N. Kaya, T. Shen, S. G. Lu, F. L. Zhao, S. Herness, *Am. J. Physiol. Regul. Integr. Comp. Physiol.* **286**, R649 (2004).
3. P. A. Davies *et al.*, *Nature* **397**, 359 (1999).
4. K. P. Zeitz *et al.*, *J. Neurosci.* **22**, 1010 (2002).
5. X. Bo *et al.*, *Neuroreport* **10**, 1107 (1999).
6. R. A. North, *Physiol. Rev.* **82**, 1013 (2002).
7. W. Rong *et al.*, *J. Neurosci.* **23**, 11315 (2003).
8. D. A. Cockayne *et al.*, *J. Physiol.* **567** (Pt. 2), 621 (2005).
9. A. M. Peier *et al.*, *Cell* **108**, 705 (2002).
10. Materials and methods and supplementary figures are available as supporting material on *Science* Online.
11. J. D. Dickman, D. V. Smith, *Brain Res.* **450**, 25 (1988).
12. D. V. Smith, T. Hanamori, *J. Neurophysiol.* **65**, 1098 (1991).
13. T. E. Finger *et al.*, *Proc. Natl. Acad. Sci. U.S.A.* **100**, 8981 (2003).
14. A. Sbarbati *et al.*, *J. Comp. Neurol.* **475**, 188 (2004).
15. M. I. Harrer, S. P. Travers, *Brain Res.* **711**, 125 (1996).
16. S. P. Travers, *Am. J. Physiol. Regul. Integr. Comp. Physiol.* **282**, R1798 (2002).
17. M. A. Barry, *J. Histochem. Cytochem.* **40**, 1919 (1992).
18. T. Iwayama, O. Nada, *Exp. Cell Res.* **46**, 607 (1967).
19. D. L. Bartel, S. Sullivan, E. Lavoie, J. Sévingy, T. E. Finger, *Chem. Senses,* in press.
20. M. S. Herness, *Neuroscience* **33**, 411 (1989).
21. T. Shen *et al.*, *Neuroscience* **130**, 229 (2005).


22. We thank D. A. Cockayne and Roche Palo Alto (Palo Alto, CA) for valuable discussion of this contribution and for graciously permitting use of the $P2X_2/P2X_3^{Dbl-/-}$ (KO) and $P2X_2/P2X_3^{Dbl+/+}$ (WT) mice. Similarly, we thank A. Basbaum and D. Julius of University of California at San Francisco for providing 5-$HT_{3A}$ receptor knockout animals, R. Margolskee of Mt. Sinai School of Medicine for use of the gustducin-GFP mice, and E. Delay (University of Vermont) for help with statistical analysis. This work was supported by grants from NIH National Institute on Deafness and Other Communication Disorders R01 DC06070, R01 DC00766, and P30 DC04657.


**Supporting Online Material**
www.sciencemag.org/cgi/content/full/310/5753/1495/DC1
Materials and Methods
Figs. S1 and S2
References and Notes

4 August 2005; accepted 1 November 2005
10.1126/science.1118435

# Chromosome Alignment and Segregation Regulated by Ubiquitination of Survivin

**Queenie P. Vong,[1]* Kan Cao,[1,2]* Hoi Y. Li,[1]† Pablo A. Iglesias,[3]‡ Yixian Zheng[1,2]‡**

**Proper chromosome segregation requires the attachment of sister kinetochores to microtubules from opposite spindle poles to form bi-oriented chromosomes on the metaphase spindle. The chromosome passenger complex containing Survivin and the kinase Aurora B regulates this process from the centromeres. We report that a de-ubiquitinating enzyme, hFAM, regulates chromosome alignment and segregation by controlling both the dynamic association of Survivin with centromeres and the proper targeting of Survivin and Aurora B to centromeres. Survivin is ubiquitinated in mitosis through both $Lys^{48}$ and $Lys^{63}$ ubiquitin linkages. $Lys^{63}$ de-ubiquitination mediated by hFAM is required for the dissociation of Survivin from centromeres, whereas $Lys^{63}$ ubiquitination mediated by the ubiquitin binding protein Ufd1 is required for the association of Survivin with centromeres. Thus, ubiquitinaton regulates dynamic protein-protein interactions and chromosome segregation independently of protein degradation.**

Mitosis is one of the visually most dynamic cellular processes, requiring a continuous assembly and disassembly of many protein complexes. We studied the chromosome passenger protein Survivin, which exhibits a dynamic interaction with centromeres (*1*–*3*). To identify proteins that interact with Survivin and thus may regulate the dynamic binding of Survivin to centromeres, we raised rabbit polyclonal antibodies to *Xenopus* Survivin (*4*). The antibody immunoprecipitated Survivin and seven other proteins from *Xenopus* egg extracts (p1 to p7) (fig. S1A). Western blotting revealed that two components of the chromosome passenger complex, inner centromere protein (INCENP) and the protein kinase Aurora B, were immunoprecipitated by the Survivin antibody.

We micro-sequenced the proteins corresponding to p1, p4, p5, and p7 (fig. S1A). Protein p1 is a homolog of the human protein USP9x (an X-linked ubiquitin specific protease, Genbank accession number NP004643) (*5*, *6*) and a mouse protein, FAM (fat facet in mouse, accession number P70398) (*7*), which share ~98% amino acid identity with one another. FAM and USP9x are homologs of the *Drosophila* protein faf (fat facet), which is required for cellularization in early embryos and for cell-fate determination in the *Drosophila* eye (*8*). Little is known about the function of USP9x, but both faf and FAM function as deubiquitinating (Dub) enzymes and can regulate protein trafficking (*9*–*14*). We refer to the *Xenopus* protein as xFAM and the human USP9x as hFAM. The proteins corresponding to p4, p5, and p7 were identified as the p97 adenosine triphosphatase associated with various cellular activities (AAA ATPase), the nuclear protein localization 4 (Npl4), and the ubiquitin fusion degradation 1 (Ufd1), respectively. The p97 protein forms a homohexameric ring that interacts with the Npl4-Ufd1 heterodimer. The resulting complex functions as a ubiquitin-selective chaperone to regulate protein ubiquitination and degradation (*15*, *16*).

Because all four proteins that coimmunoprecipitated with Survivin are involved in the ubiquitin-mediated signaling, we reasoned that

[1]Department of Embryology, Carnegie Institution of Washington and Howard Hughes Medical Institute, 3520 San Martin Drive, Baltimore, MD 21218, USA. [2]Department of Biology and [3]Department of Electrical and Computer Engineering, Johns Hopkins University, Baltimore, MD 21218, USA.

*These authors contributed equally to this work.
†Present address: School of Biological Sciences, Nanyang Technological University, Singapore 637515.
‡To whom correspondence should be addressed. E-mail: pi@jhu.edu (P.A.I.); zheng@ciwemb.edu (Y.Z.)

Survivin function in mitosis might be regulated by ubiquitination. To test this idea, we focused on the de-ubiquitinating enzyme hFAM. We generated five antibodies to hFAM, with four peptides and a fusion protein as antigens (fig. S1B) (*4*). All five antibodies recognized hFAM and xFAM by Western blotting and by immunoprecipitation (fig. S1, C and D). Reciprocal immunoprecipitation confirmed that xFAM and *Xenopus* Survivin interacted with one another in *Xenopus* egg extracts (fig. S1E). Furthermore, Myc-tagged human Survivin immunoprecipitated with hFAM from HeLa cells (fig. S1F). None of our affinity-purified hFAM antibodies revealed specific localization of hFAM in HeLa cells or mouse NIH 3T3 cells, suggesting that FAM is evenly distributed in these cells.

We inhibited the expression of hFAM in HeLa cells with two small interfering RNAs (siRNAs) (hFAM-s1 or hFAM-s2). A Survivin siRNA (*17*) and luciferase siRNA were used as controls (*18*). Western blotting revealed that siRNAs of hFAM and Survivin decreased the expression of proteins, whereas the control luciferase siRNA had no effect on either protein (Fig. 1A). Decreased expression of either hFAM or Survivin inhibited cell proliferation (Fig. 1B). However, decreased expression of hFAM did not affect the expression of Survivin or vice versa (Fig. 1A). Thus, hFAM appears not to regulate the stability of Survivin. Decreased expression of either Survivin or hFAM resulted in an increase in misaligned chromosomes in metaphase and lagging chromosomes in anaphase (Fig. 1C). (We defined misaligned chromosomes in metaphase as chromosomes that failed to align with the majority of chromosomes at metaphase plates.) Furthermore, 4′,6′-diamidino-2-phenylindole (DAPI) staining revealed that down-regulation of hFAM or Survivin led to an increase of binucleated or multinucleated cells from ~5% in control to ~12% in hFAM RNA interference (RNAi)–treated cells and ~50% in Survivin RNAi-treated cells (Fig. 1D), suggesting that hFAM has a minor role, if any, in cytokinesis, compared with that of Survivin. Decreased expression of FAM in NIH 3T3 cells with hFAM-s1 treatment (hFAM-s1 sequence is identical in mouse) also caused similar defects in cell division.

The cell-division defects observed after inhibition of hFAM expression were largely rescued by the expression of a FAM molecule mutagenized at three wobble codons, resulting in a FAM gene that encodes wild-type (WT) protein ($pFAM^{INS}$) and is insensitive to the siRNA. But, the defects were not fixed by expressing the nonmutagenized $FAM^{WT}$ (*4*) (Fig. 1E and fig. S1G). Thus, hFAM, like Survivin, regulates chromosome alignment and segregation in mitosis.

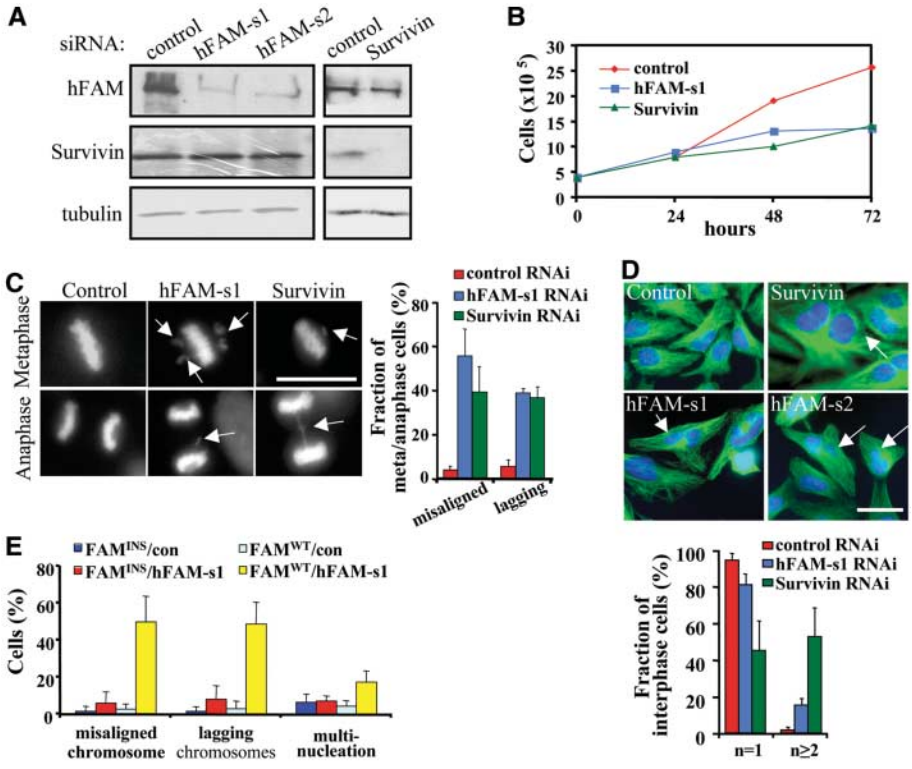


**Fig. 1.** hFAM characterization. (**A**) Western blotting of HeLa cells treated with siRNAs corresponding to luciferase (control), hFAM (hFAM-s1 or hFAM-s2), and Survivin. Survivin and hFAM were down-regulated ~80% by their respective siRNAs. Western blotting of tubulin served as loading controls. (**B**) Down-regulation of hFAM or Survivin by their respective siRNAs reduced cell proliferation as compared to the control siRNA treatment. (**C**) Accumulation of misaligned and lagging chromosomes in metaphase and anaphase after depletion of hFAM or Survivin, respectively. HeLa cells treated with the indicated siRNA were stained by DAPI (left). The percentages of mitotic cells with misaligned or lagging chromosomes in metaphase or anaphase, respectively, were quantified (right). (**D**) Accumulation of bi-nucleated or multinucleated cells after depletion of hFAM or Survivin. HeLa cells (top) treated with the indicated siRNA were stained with antibody to tubulin (green) and DAPI (blue). Arrows point to cells with more than one nucleus. The percentages of interphase cells with single ($n = 1$) or more ($n \geq 2$) nuclei were quantified (bottom). (**E**) Cell-division defects were caused by depletion of hFAM. Expression of $FAM^{INS}$ significantly reduced the defects caused by hFAM RNAi-treatment. Error bars indicate standard deviation (SD) from at least three independent experiments. For chromosome segregation defects, 100 mitotic cells were analyzed for each RNAi experiment. Scale bars in (C) and (D), 20 μm.

We tested whether hFAM regulates Survivin binding to centromeres in mitosis. Centromeres were detected using the anti-centromere antibody (ACA) that recognizes several centromere proteins (*19*), and Survivin was detected with Survivin antibodies. ACA staining of centromeres appeared as bright dots in both control and hFAM RNAi-treated cells (Fig. 2, A and B) (*20*). However, although the overall Survivin levels on the prometaphase chromosomes or metaphase-aligned chromosomes were similar in control or hFAM RNAi-treated cells, Survivin staining of centromeres appeared more diffuse in hFAM RNAi-treated cells (Fig. 2, A and B).

In prometaphase control cells, most focused ACA-stained dots corresponded to strongly focused Survivin dots. In contrast, in cells treated with hFAM siRNA, many focused ACA dots did not correspond to focused Survivin dots (Fig. 2, A and C). In metaphase control cells, Survivin dots were flanked by pairs of ACA dots on centromeres of chromosomes aligned at the metaphase plate. However, in hFAM RNAi-treated cells, the majority of focused ACA dots did not flank Survivin dots (Fig. 2, B and C). Double immunostaining with antibodies to ACA and Aurora B revealed similar defects of Aurora B localization in hFAM RNAi-treated cells. Thus, the depletion of hFAM disrupted normal localization of Survivin, which could lead to chromosome misalignment and segregation.

We also examined Survivin localization on the misaligned chromosomes. Survivin staining on these chromosomes was brighter at the centromeres and appeared to spread into chromosome arms in hFAM RNAi-treated cells, compared with the staining on rare misaligned chromosomes in controls (Fig. 2D). Quantification revealed an approximate twofold increase in total Survivin stain-

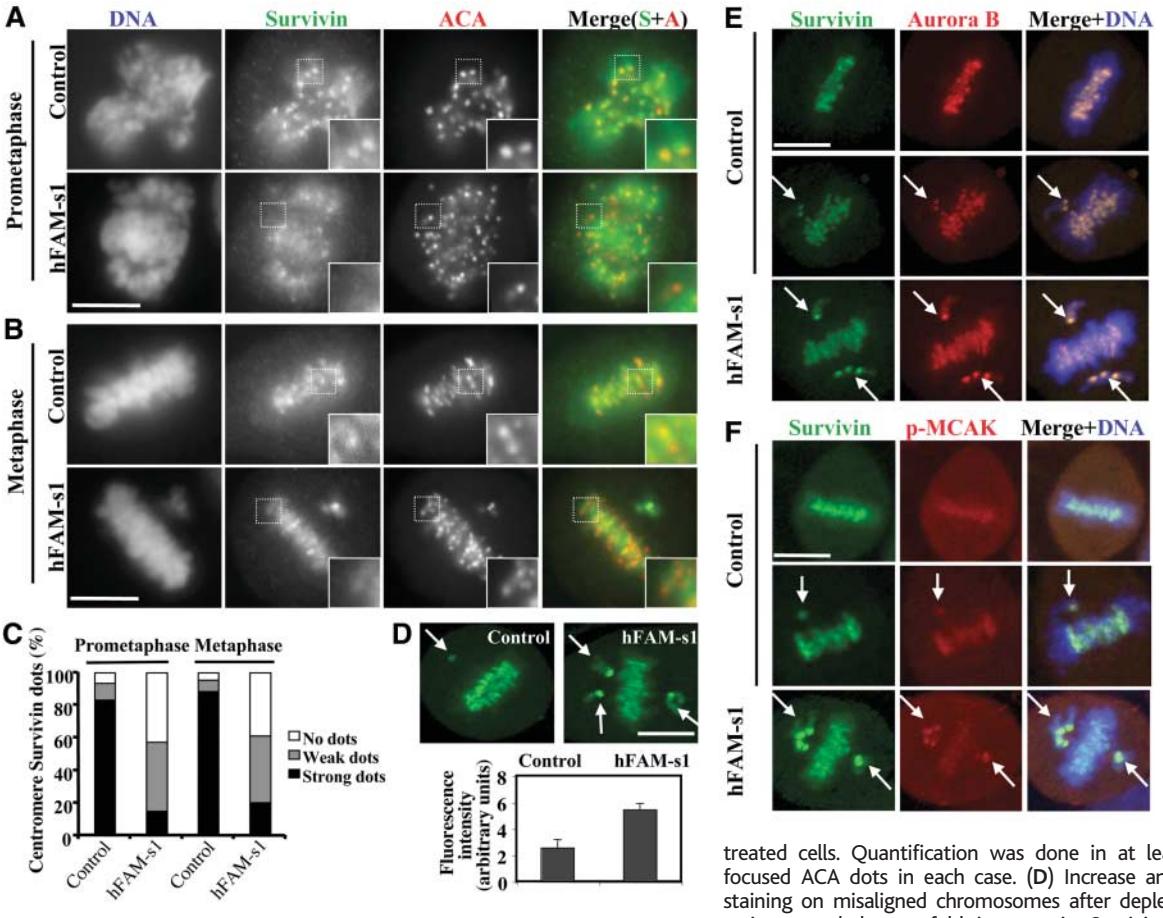


**Fig. 2.** Regulation by hFAM of the localization of Survivin and Aurora B to centromeres in mitosis. (**A** and **B**) Survivin in prometaphase (A) and metaphase (B) cells treated with or without hFAM-s1. HeLa cells were stained by DAPI (DNA) and by antibodies to Survivin (green) and ACA (red). The images were taken by focusing on ACA-positive dots. Focused ACA dots and their corresponding areas in the Survivin-staining channel are highlighted by squares and enlarged in the right corners of each image. (**C**) Reduced number of centromeres with focused Survivin staining after depletion of hFAM. Percentages of centromeres (identified as focused ACA dots) having no, weak, or strong dots of Survivin were quantified in control and hFAM RNAi-treated cells. Quantification was done in at least 10 cells with ~100 focused ACA dots in each case. (**D**) Increase and expansion of Survivin staining on misaligned chromosomes after depletion of hFAM. Quantification revealed ~twofold increase in Survivin staining on misaligned chromosomes in hFAM RNAi-treated cells, compared with controls. Error bars indicate SD from >42 cells. (**E**) Increased and expanded staining of Aurora B on centromeres of misaligned chromosomes after hFAM depletion. (**F**) Aurora B phosphorylation of MCAK (p-MCAK) at the centromeres of misaligned chromosomes after hFAM depletion. Arrows in panels point to misaligned chromosomes. Scale bars, 10 μm.

ing on the misaligned chromosomes in hFAM RNAi-treated cells, compared with that in control cells (Fig. 2D). Aurora B staining was also expanded beyond centromeres on the misaligned chromosomes in hFAM RNAi-treated cells (Fig. 2E).

Phosphorylation of the mitotic centromere-associated kinesin (MCAK) by Aurora B inhibits MCAK's ability to depolymerize microtubules at the kinetochore (*21*, *22*). The balance between phosphorylation of MCAK by Aurora B and dephosphorylation by phosphatase I at kinetochores is thought to allow proper microtubule attachment to kinetochores. Thus, excess accumulation of Survivin and Aurora B on misaligned chromosomes of hFAM RNAi-treated cells might increase MCAK phosphorylation at kinetochores, which might prevent MCAK from correcting chromosome misalignment. Indeed, immunostaining with an antibody that recognizes Aurora B–phosphorylated MCAK (*21*) showed an increased accumulation of phospho-MCAK on misaligned centromeres in hFAM RNAi-treated cells compared with those in controls (Fig. 2F and fig. S2). Thus, hFAM regulates Survivin, which in turn regulates MCAK phosphorylation by Aurora B at the centromeres.

We found no obvious difference in the localization of Survivin and Aurora B to central spindles in anaphase and midbodies in telophase in hFAM RNAi-treated cells (fig. S3), suggesting that hFAM specifically regulates the chromosome-segregation function, but not the cytokinesis function, of Survivin. The bi-nucleation or multinucleation in hFAM RNAi-treated cells (Fig. 1D) may result from lagging chromosomes that block the closure of cytokinesis furrows.

We used both fluorescence recovery after photobleaching (FRAP) and fluorescence loss in photobleaching (FLIP) to measure the binding kinetics of Survivin to centromeres in mitosis (*23*). Control treatment or hFAM RNAi treatment was applied to HeLa cells that were transiently expressing Survivin–green fluorescent protein (GFP) (*24*). Expression of Survivin-GFP can rescue HeLa cells from Survivin RNAi (*25*), so we presumed that Survivin-GFP could be used to report the behavior of endogenous Survivin (fig. S4). Using FRAP, we found that in control RNAi cells, the half-time ($t_{1/2}$) of Survivin-GFP recovery was 2 to 6 s (*3*). However, the $t_{1/2}$ for Survivin-GFP recovery in hFAM RNAi-treated cells was increased to 80 to 100 s on prometaphase and metaphase chromosomes (Fig. 3, A and B, and fig. S5) (*26*). There was also an increase in the immobile fraction of Survivin on the misaligned centromeres (table S3). Survivin-GFP on misaligned metaphase chromosomes had a slower recovery than that on aligned chromosomes in hFAM RNAi-treated cells (Fig. 3B). Using FLIP, we found that Survivin-GFP dissociated from centromeres faster in control RNAi cells than in hFAM RNAi-treated cells in both prometaphase and metaphase (Fig. 3 C and D, and fig. S5) (*26*). Furthermore, in hFAM RNAi-treated cells, Survivin-GFP on the misaligned chromosomes dissociated more slowly than that on aligned chromosomes (Fig. 3C and table S3). This slower dissociation is consistent with the observation of an increased accumulation of Survivin on misaligned chromosomes in hFAM RNAi-treated cells (Fig. 2D). Thus, hFAM appears to control centromeric localization of Survivin by regulating the dynamic dissociation of Survivin from centromeres. Survivin-GFP at central spindles

and midbodies exhibited similar FRAP behavior in control and in hFAM RNAi-treated cells (fig. S6), consistent with the idea that hFAM does not regulate the cytokinesis function of Survivin.

Because polyubiquitination through Lys$^{63}$ (K63) of ubiquitin regulates protein-protein interactions but not protein degradation (*27*), we tested whether hFAM might regulate the dynamic interaction of Survivin with centromeres by controlling the level of K63 ubiquitination on Survivin. We characterized Survivin ubiquitination in mitosis in HeLa cells transfected with Myc-tagged Survivin, wild-type hemagglutinin (HA)–tagged ubiquitin, or mutant HA-tagged ubiquitins that mediate only K48 or K63 linkages. Myc-tagged Survivin was analyzed by immunoprecipitation and Western blotting (*28*). Survivin was ubiquitinated through K63 and K48 linkages in mitosis, and the ubiquitination was not caused by mitotic arrest (fig. S7, A and B). Furthermore, the expression of a FAM fragment possessing the Dub catalytic domain and Dub activity (V5FAM$^{CAT}$, fig. S1B) (*13*, *14*) reduced the wild-type (contains both K63 and K48 linkages) and the K63-linked ubiquitin on Survivin to about half of the controls. However, the K48-linked ubiquitination was not affected (Fig. 4A and fig. S7C). The modest reduction of ubiquitination reflects the modest expression of V5FAM$^{CAT}$ (fig. S7C). We were unable to overexpress either FAM$^{CAT}$ or full length FAM in cells.

The expression of pV5FAM$^{CAT}$ in cells treated with hFAM-s1 (hFAM-s1 is upstream of the V5FAM$^{CAT}$ fragment, fig. S1B) led to a reduction of misaligned and lagging chromosomes and of bi-nucleated or multinucleated cells (Fig. 4B). Thus hFAM RNAi appears to increase the amount of K63-linked ubiquitination on Survivin, which disrupts accurate targeting of Survivin to centromeres, leading to chromosome misalignment and missegregation in mitosis.

Because hFAM RNAi caused cell death, we were unable to assay K63 ubiquitination on Survivin after exposing cells to hFAM RNAi. Therefore, we sought to study the effect of K63 ubiquitination on Survivin by mutagenizing the lysines (K) to arginines (R) on Survivin. K residues in proteins are involved in a number of posttranslational modifications including ubiquitination, sumoylation, methylation, and acetylation. Because posttranslational modifications of different K residues in a protein could regulate one another (*29*), it may be possible to create Survivin mutants that have increased or decreased K63 ubiquitination. There are 16 K residues in human Survivin. Nine of these (K23, K62, K78, K79, K90, K91, K110, K112, and K115) are highly conserved. On the basis of the crystal structure of Survivin, four of these nine Ks (K23, K62, K78, and K79) are clustered in the N terminus of Survivin that forms the Bir [baculovirus Ile-Ala-Pro (IAP) repeat] domain, whereas the remaining five Ks (K90, K91, K110, K112, and K115) are clustered in the C terminus (*30*).

We mutagenized all 16 Ks into Rs, but this mutant Survivin was not expressed in cells. Even when only the nine conserved Ks were changed to Rs, the mutant Survivin expression level was still too low to allow determination of its localization in cells. Survivin mutant (Sur4K-R) with four Ks (K23, K62, K78, and K79) changed to Rs was expressed and bound to centromeres (Fig. 4C). However, not every centromere (identified by ACA) had clear Sur4K-R localization (fig. S8, A and B). Ubiquitination assays revealed that, compared with wild-type Survivin, cells expressing Sur4K-R had increased ubiquitination that was mostly accounted for by the K63 linkage (Fig. 4D).

We also used FRAP to study the interaction between Sur4K-R and centromeres. Sur4K-R-GFP or wild-type Survivin (Sur-GFP) was transfected into HeLa cells for FRAP analysis. Sur4K-R-GFP showed reduced FRAP compared with that of Sur-GFP

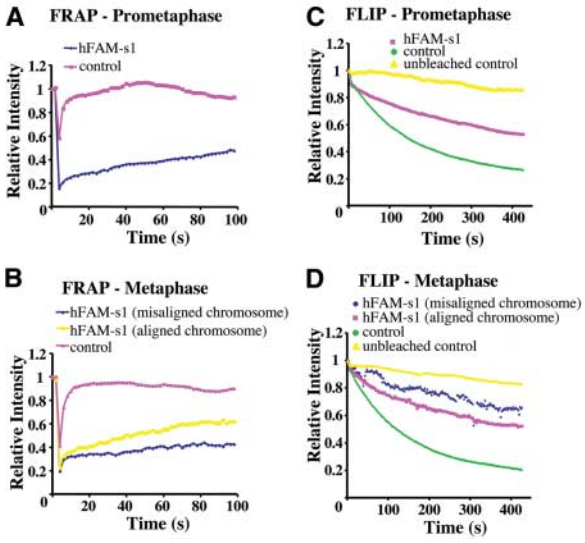


**Fig. 3.** Regulation by hFAM of the dynamic turnover of Survivin on mitotic centromeres. (**A** and **B**) FRAP analyses of Survivin-GFP in prometaphase (A) and metaphase (B) cells treated with either hFAM-s1 or control siRNA. (**C** and **D**) FLIP analyses of Survivin-GFP in prometaphase (C) and metaphase (D) cells. FLIP was quantified by plotting the loss of Survivin-GFP on all prometaphase chromosomes or aligned metaphase chromosomes over time in both control and hFAM RNAi-treated cells. FLIP on the misaligned chromosomes in metaphase was also quantified in hFAM RNAi-treated cells. The FLIP and FRAP curves show averages of at least six independent experiments.

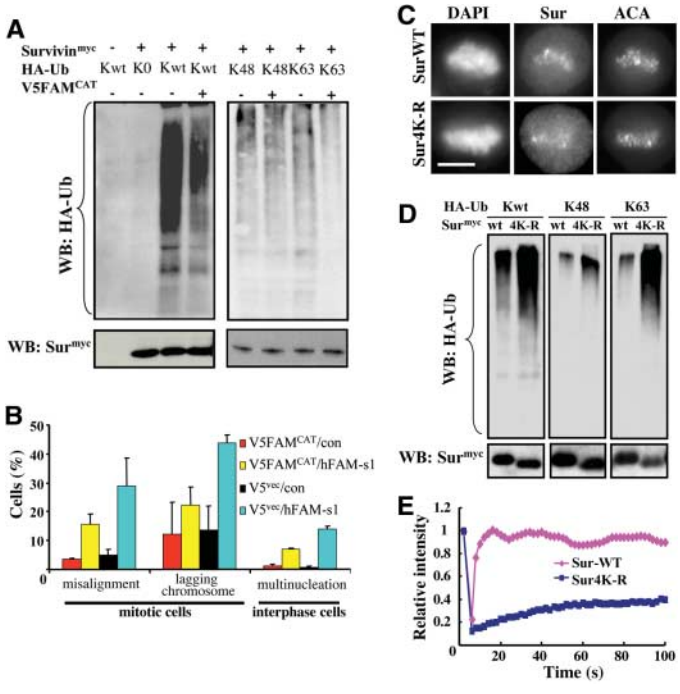


**Fig. 4.** Deubiquitination of Survivin by hFAM. (**A**) Effect of V5FAM$^{CAT}$ on wild-type, K63-, or K48-ubiquitination of Survivin. (**B**) Effect of V5FAM$^{CAT}$ on cell-division defects caused by hFAM-s1. Vector control (pV5$^{vec}$) or pV5FAM$^{CAT}$ were used to transfect HeLa cells treated with control siRNA (con) or hFAM-s1. Error bars indicate SD from at least three independent experiments. (**C**) Localization of Survivin. Mutant Survivin (Sur4K-R$^{Myc}$) or wild-type Survivin$^{Myc}$ were transfected into HeLa cells. Survivin, centromeres, or DNA were detected using antibody to either Myc or ACA, or DAPI, respectively. (**D**) Ubiquitination assay of wild-type Survivin and Sur4K-R. (**E**) FRAP. Sur4K-R was subcloned into pEGFP-N3 to make Sur4K-R-GFP. FRAP analyses were carried out in cells expressing either Sur4K-R-GFP or wild-type Sur-GFP. The FRAP curves show averages from at least six different cells.

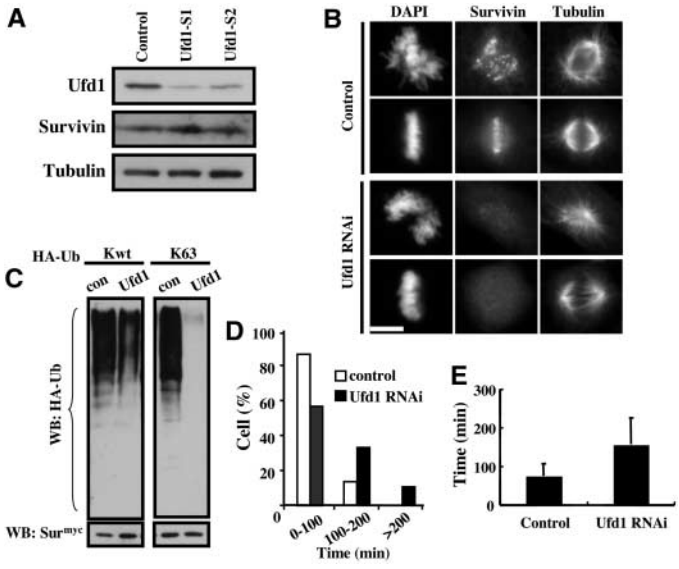


**Fig. 5.** Regulation of Survivin by Ufd1. (**A**) Depletion of Ufd1 by two different siRNAs (Ufd1-S1 or Ufd1-S2) did not change Survivin protein expression level. Tubulin served as loading controls. (**B**) Ufd1-regulated binding of Survivin to centromeres. Control or Ufd1 RNAi-treated cells were processed for immunofluorescence to detect DNA, Survivin, and microtubules. Representative prometaphase and metaphase cells are shown. (**C**) Ufd1 regulates K63 ubiquitination of Survivin. Survivin ubiquitination by either wild-type ubiquitin (Kwt) or mutant ubiquitin (K63) was analyzed in cells treated with either control (con) or Ufd1 RNAi. (**D**) Regulation of mitotic progression by Ufd1. Cells were treated with control or Ufd1 siRNA for 48 hours followed by imaging on a temperature-controlled stage at 3-min intervals for 12 to 16 hours using a Hoffman modulation contrast objective lens (10×) on a Nikon TE200 microscope equipped with an Orca-2 camera. The graph shows quantification of elapsed time for cells that progressed from round-up to chromosome separation. At least 50 mitotic cells were analyzed in either control or Ufd1 RNAi-treatment. (**E**) Chromosome alignment regulated by Ufd1. HeLa cells stably expressing GFP-H2B were treated with control or Ufd1 siRNA for 48 hours followed by imaging at 3-min intervals for 12 to 16 hours using a fluorescence objective lens (20×). The graph shows quantification of time elapsed in prometaphase and metaphase in control or Ufd1 RNAi-treated cells. Control cells spent shorter time to achieve metaphase chromosome alignment than did Ufd1 RNAi-treated cells (*t* test, $P < 0.01$). Error bars indicate SD. Scale bar, 10 μm.

(Fig. 4E and fig. S8C). The FRAP kinetics of Sur4K-R-GFP (Fig. 4E) were similar to those of wild-type Sur-GFP in hFAM RNAi-treated cells (Fig. 3, A and B).

The above studies indicate that excessive K63 ubiquitination of Survivin blocks its dissociation from centromeres. Thus, insufficient K63 ubiquitination might inhibit the binding of Survivin to centromeres. The p97-Ufd1-Npl4 complex, which co-immunoprecipitated with Survivin and FAM (fig. S1A), recruits ubiquitin ligase to substrates to extend the ubiquitin chains on the substrates (*16*). This complex regulates spindle disassembly at the end of mitosis (*15*), and we reasoned that it might have an earlier mitotic role by promoting K63 ubiquitination of Survivin and chromosome alignment.

We verified the interaction between Survivin and the complex in HeLa cells expressing V5-tagged Ufd1 and Myc-tagged Survivin (fig. S9A). Then we used siRNAs directed at different regions of Ufd1 (Ufd1-S1 or Ufd1-S2) to disrupt the function of the p97-Ufd1-Npl4 complex (*18*). The depletion of Ufd1 by either siRNA did not affect Survivin protein levels (Fig. 5A).

Both siRNAs had similar effects. Decreased expression of Ufd1 did not block bipolar spindle assembly (Fig. 5B) (*15*), but it consistently reduced the K63 ubiquitination of Survivin (Fig. 5C). The partial reduction of the total ubiquitination of Survivin, as assayed with wild-type ubiquitin, can be accounted for by the reduction in K63-linked ubiquitination (Fig. 5C). The effect of Ufd1 down-regulation on K48 ubiquitination of Survivin was variable, ranging from no effect to mild reduction. Thus, Ufd1 appears to be required primarily for K63 ubiquitination of Survivin in mitosis.

Immunofluorescence microscopy revealed that Survivin staining of centromeres was either absent or reduced in cells treated with Ufd1 RNAi (Fig. 5B). We stained the centromeres with Survivin and ACA antibodies. Ufd1 RNAi did not affect ACA staining of centromeres (fig. S9B). Whereas over 80% of centromeres had strong Survivin staining in control RNAi-treated cells, less than 10% of centromeres had strong Survivin staining in Ufd1 RNAi-treated cells (fig. S9C). Aurora B staining of centromeres was also absent or reduced in the Ufd1 RNAi-treated cells (fig. S9D). Thus, K63 ubiquitination of Survivin appears to be required for centromere targeting.

We imaged cell division in live control or Ufd1 RNAi-treated cells by Hoffman modulation contrast. Metaphase chromosomes appear as a distinctive bar at the middle of the cell, and the metaphase-anaphase transition can be clearly detected when the metaphase chromosomal bar splits into two (fig. S9E). We quantified the time elapsed from the beginning of mitosis (judged by cell round-up) to the time when the metaphase chromosome bar separated into two in control and Ufd1 RNAi-treated cells. The Ufd1 RNAi-treated cells took a longer time to complete chromosome segregation (Fig. 5D). This observation suggests that Ufd1 RNAi-treated cells have difficulty in achieving chromosome alignment in mitosis.

To further determine whether the lack of Survivin at centromeres affected chromosome alignment, we imaged chromosomes in HeLa cells expressing GFP-histone H2B. Many Ufd1 RNAi-treated cells took longer to achieve metaphase chromosome alignment (fig. S9F). Quantification revealed that the time cells spent in prometaphase and metaphase was significantly longer in the Ufd1 RNAi-treated cells than in control cells (Fig. 5E). Thus, Survivin ubiquitination on K63 is required for its centromere targeting and chromosome alignment in mitosis.

Ubiquitin has a well-established role in targeting proteins for degradation. However, it also regulates DNA repair (*31*) and nuclear factor κB (NF-κB) signaling (*32*) in a protein degradation–independent manner. Our studies reveal that the protein degradation–independent signaling of ubiquitination is important in regulating dynamic protein targeting in mitosis. Degradation of Survivin by proteasomes is controlled by K48-linked ubiquitination at the end of mitosis (*33*). We propose that a balanced K63-linked ubiquitination and deubiquitination of Survivin is necessary for the correct targeting of Survivin and other chromosome passenger proteins to centromeres in mitosis. This in turn regulates a balanced phosphorylation and dephosphorylation of MCAK and chromosome alignment. Many ubiquitin ligases, Dubs, and their regulators have been identified in eukaryotic genomes (*34*, *35*). These proteins may have far-reaching roles in regulating dynamic protein-protein interactions in mitosis that are independent of protein degradation.

### References and Notes

1. M. Carmena, W. C. Earnshaw, *Nat. Rev. Mol. Cell Biol.* **4**, 842 (2003).
2. P. D. Andrews, E. Knatko, W. J. Moore, J. R. Swedlow, *Curr. Opin. Cell Biol.* **15**, 672 (2003).
3. V. Beardmore, L. Ahonen, G. Gorbsky, M. Kallio, *J. Cell Sci.* **117**, 4033 (2004).
4. Human Survivin was C-terminally tagged with the Myc-epitope or enhanced GFP (EGFP) using pEF6/Myc-His or pEGFP-N3 (Invitrogen), respectively. Point mutations of Survivin were made using Myc-tagged Survivin and subcloned into pEGFP-N3. The expression constructs for V5FAM and HA-ubiquitin were described previously (*14*, *35*). The pV5FAM$^{CAT}$ expression construct was made by subcloning the FAM fragment (amino acids 1212 to 2410) into the BamHI site of the pEF6/V5-His expression vector (Invitrogen). pV5FAM$^{INS}$ was made by changing wobble codons (GCA GTT AGC GGG TGG AAG, changed nucleotides are in bold) corresponding to hFAM-s1 siRNA sequence using GeneEditor (Promega). Antibody to *Xenopus* Survivin

was raised against glutathione S-transferase (GST) *Xenopus* Survivin and affinity purified using cleaved Survivin. Antibodies against hFAM were raised against each of four peptides (TPPDEQGQGDAPPQLED, CAPDEHESPPPEDAP, QRAQENYEGSEEVSPPQTKDQ, and GDEKQDNESNVDPRDDV) (*36*) and one GST fusion of the C-terminal fragment (amino acids 2347 to 2547) of hFAM. All were affinity purified against the respective antigens. Mouse Ufd1 was cloned into the pEF6/V5-His vector. Ufd1 antibodies were raised against GST-Ufd1 fusion protein and purified against His-tagged Ufd1. Antibodies against tubulin (Sigma), ACA (Antibodies Incorporated), human Survivin (R&D systems), human Aurora B (BD Biosciences), HA (Roche), Myc (Santa Cruz), and control immunoglobulin G (IgG) (Jackson Laboratory) were purchased. Antibodies against phosphorylated MCAK were described previously (*21*). Immunoprecipitation and immunofluorescence were carried out as described previously (*15*).

5. M. Jones *et al.*, *Hum. Mol. Genet.* **5**, 1695 (1996).
6. T. Noma *et al.*, *Mech. Dev.* **119S**, S91 (2002).
7. S. Wood *et al.*, *Mech. Dev.* **63**, 29 (1997).
8. J. Fischer-Vize, G. Rubin, R. Lehmann, *Development* **116**, 985 (1992).
9. Y. Huang, J. Fischer-Vize, *Development* **122**, 3207 (1996).
10. X. Chen, B. Zhang, J. Fischer, *Genes Dev.* **16**, 289 (2002).
11. A. Cadavid, A. Ginzel, J. Fischer, *Development* **127**, 1727 (2000).
12. Z. Wu, Q. Li, M. Fortini, J. Fischer, *Dev. Genet.* **25**, 312 (1999).
13. S. Taya *et al.*, *J. Cell Biol.* **142**, 1053 (1998).
14. R. Murray, L. Jolly, S. Wood, *Mol. Biol. Cell* **15**, 1591 (2003).
15. K. Cao, R. Nakajima, H. H. Meyer, Y. Zheng, *Cell* **115**, 355 (2003).
16. H. Richly *et al.*, *Cell* **120**, 73 (2005).
17. A. Carvalho, M. Carmena, C. Sambade, W. C. Earnshaw, S. P. Wheatley, *J. Cell Sci.* **116**, 2987 (2003).
18. RNA interference was carried out by transfecting HeLa, NIH 3T3, or human HEK 293 cells with 160 to 200 nM (final) siRNA (Dharmacon or Qiagen) corresponding to luciferase (CGTACGCGGAATACTTCGA), Survivin (GGACCACCGCATCTCTACA), hFAM (hFAM-s1: GCAGTGAGTGGCTGGAAG or hFAM-s2: ACTTCCTACCGAATGCAGA), or Ufd1 (Ufd1-S1: CTGGGCTACAAAGAACCCGAA or Ufd1-S2: CTGCGTGTGATGGAGACCAAA) (*36*) using Oligofectamine (Invitrogen). The cells were analyzed at 48 or 72 hours after transfection. For hFAM rescue experiments, HeLa cells were transfected with $pV5FAM^{INS}$, $pV5FAM^{WT}$, $pV5FAM^{CAT}$, or pV5 vector for at least 48 hours before siRNA transfection. Cells were analyzed 72 hours after siRNA transfection.
19. W. Earnshaw, B. Bordwell, C. Marino, N. Rothfield, *J. Clin. Invest.* **77**, 426 (1986).
20. R. Gassmann *et al.*, *J. Cell Biol.* **166**, 179 (2004).
21. P. Andrews *et al.*, *Dev. Cell* **6**, 253 (2004).
22. W. Lan *et al.*, *Curr. Biol.* **14**, 273 (2004).
23. H. Li, D. Wirtz, Y. Zheng, *J. Cell Biol.* **160**, 635 (2003).
24. HeLa cells were treated with hFAM-s1 or control siRNA for ~24 hours and then transfected with Survivin-GFP. FLIP or FRAP was carried out 48 to 72 hours after transfection. Detailed descriptions of the kinetic modeling of FLIP and FRAP can be found in (*26*).
25. M. Delacour-Larose, A. Mollar, D. A. Skoufias, R. L. Margolis, S. Dimitrov, *Cell Cycle* **3**, 1418 (2004).
26. Materials and methods are available as supporting materials on *Science* Online.
27. L. Sun, Z. Chen, *Curr. Opin. Cell Biol.* **16**, 119 (2004).
28. For ubiquitination assays, HeLa cells or HEK 293 cells were cotransfected with Myc-Survivin and HA-ubiquitin or the respective vector controls for 30 hours followed by nocodazole (400 nM final) arrest. Cell lysates were subjected to immunoprecipitation using antibody to Myc. Ubiquitinated Myc-Survivin was detected using antibody to HA. To assay the Dub activity of FAM, HeLa cells were cotransfected with Myc-Survivin, HA-ubiquitin, and $V5FAM^{CAT}$ or the respective vector controls followed by the same treatment and analyses described above.
29. X. J. Yang, *Oncogene* **3**, 653 (2005).
30. M. A. Verdecia *et al.*, *Nat. Struct. Biol.* **7**, 602 (2000).
31. C. Hoege, G.-L. Pfander, G. Pyrowolakis, S. Jentsch, *Nature* **419**, 135 (2002).
32. I. Wertz *et al.*, *Nature* **430**, 694 (2004).
33. J. Zhao, T. Tenev, L. Martins, J. Downward, N. Lemoine, *J. Cell Sci.* **23**, 4363 (2000).
34. C. Pickart, *Cell* **116**, 181 (2004).
35. S. Wing, *Inter. J. Biochem. Cell Biol.* **35**, 590 (2003).
36. Single-letter abbreviations for the amino acid residues are as follows: A, Ala; C, Cys; D, Asp; E, Glu; F, Phe; G, Gly; H, His; I, Ile; K, Lys; L, Leu; M, Met; N, Asn; P, Pro; Q, Gln; R, Arg; S, Ser; T, Thr; V, Val; W, Trp; and Y, Tyr.
37. We thank J. Swedlow, S. Wood, H. Meyer, and T. Dawson for antibodies and constructs; B. Lane for protein sequencing; C. Pickart for helpful advice on ubiquitination assays; O. Martin and R. Chen for excellent technical support; and M. Guo, D. Koshland, J. Yanowitz, and the members of Zheng lab for helpful comments. This work was supported by Howard Hughes Medical Institution and by National Institute of General Medical Sciences grant no. GM56312.

**Supporting Online Material**
www.sciencemag.org/cgi/content/full/310/5753/1499/DC1
Materials and Methods
Figs. S1 to S11
Tables S1 to S3
References

14 September 2005; accepted 25 October 2005
10.1126/science.1120160

# Prostaglandin $E_2$ Promotes Colon Cancer Cell Growth Through a $G_s$-Axin-β-Catenin Signaling Axis

**Maria Domenica Castellone,[1] Hidemi Teramoto,[2] Bart O. Williams,[3] Kirk M. Druey,[4] J. Silvio Gutkind[1]***

**How cyclooxygenase-2 (COX-2) and its proinflammatory metabolite prostaglandin E2 (PGE2) enhance colon cancer progression remains poorly understood. We show that PGE2 stimulates colon cancer cell growth through its heterotrimeric guanine nucleotide-binding protein (G protein)–coupled receptor, EP2, by a signaling route that involves the activation of phosphoinositide 3-kinase and the protein kinase Akt by free G protein βγ subunits and the direct association of the G protein $\alpha_s$ subunit with the regulator of G protein signaling (RGS) domain of axin. This leads to the inactivation and release of glycogen synthase kinase 3β from its complex with axin, thereby relieving the inhibitory phosphorylation of β-catenin and activating its signaling pathway. These findings may provide a molecular framework for the future evaluation of chemopreventive strategies for colorectal cancer.**

Colorectal cancer represents the third leading cause of cancer-related deaths in both men and women in the United States (*1*). The development of colon cancer results from the sequential accumulation of mutations or deletions in the coding sequence of a number of tumor-suppressor genes and oncogenes, together with aberrant activity of molecules controlling genomic stability (*2*). Patients with familial adenomatous polyposis, a disease characterized by the presence of numerous colorectal polyps, harbor germline mutations of one allele of the *adenomatous polyposis coli* (*APC*) tumor-suppressor gene and develop colon cancer upon mutational damage or loss of the wild-type allele (*3*). Like humans, mice with germline mutations in *APC*, $Apc^{min}$ (multiple intestinal neoplasia) mice, are predisposed to the formation of intestinal adenomas (*4*). Loss of full-length APC proteins is also one of the earliest events occurring in sporadic colon cancer, suggesting that APC may act as a gatekeeper of the colonic epithelium. Nonsteroidal anti-inflammatory drugs (NSAIDs)—which inhibit two enzymes involved in prostaglandin biosynthesis, cyclooxygenase-1 (COX-1) and cyclooxygenase-2 (COX-2)—reduce the number and size of adenomas in patients with familial adenomatous polyposis and prevent colon cancer development in $Apc^{min}$ mice (*5*). Indeed, emerging clinical and experimental evidence now supports a potent antitumorigenic efficacy of NSAIDs in colon cancer (*6*) and implicates the contribution of COX-2 and one of its metabolites, prostaglandin E2 (PGE2), in colon cancer development (*7*). How the

[1]Oral and Pharyngeal Cancer Branch, National Institute of Dental and Craniofacial Research, National Institutes of Health, Bethesda, MD 20892–4340, USA. [2]Kojin Hospital, 1-710 Shikenya, Moriyama, Nagoya 463-8530, Japan. [3]Laboratory of Cell Signaling and Carcinogenesis, Van Andel Research Institute, Grand Rapids, MI 49503, USA. [4]Molecular Signal Transduction Section, Laboratory of Allergic Diseases, National Institute of Allergy and Infectious Diseases, National Institutes of Health, Rockville, MD 20852, USA.

*To whom correspondence should be addressed. E-mail: sg39v@nih.gov